

PACS numbers: 07.07.Df, 68.37.Hk, 77.84.Lf, 78.20.Ci, 81.05.Qk, 81.07.Pr, 82.35.Np

## **Fabrication of Novel PEO–PVA/SrTiO<sub>3</sub>–CoO Nanostructures for Low-Cost Pressure Sensor and Gamma-Ray Shielding**

Shaimaa Mazhar Mahdi and Majeed Ali Habeeb

*College of Education for Pure Sciences,  
Department of Physics,  
University of Babylon,  
Hillah, Iraq*

Nanocomposites (NCs) are used usually for different fields in an industrial application, which require minimal cost and weight. In this study, strontium–titanium trioxide (SrTiO<sub>3</sub>)/cobalt oxide (CoO) nanoparticles (NPs) are combined with polyethylene oxide (PEO)/polyvinyl alcohol (PVA) polymer blend to create NCs. The films are made using the casting process, and different weight percentages of SrTiO<sub>3</sub>/CoO NPs (of 0, 1, 2, 3 and 4 wt.%) are added to the polymer mixture. Scanning electron microscopy shows the surfaces of the PEO/PVA/SrTiO<sub>3</sub>/CoO NCs films with several randomly distributed aggregates or fragments on the top surface consistently and coherently. Images of optical microscope demonstrate that the blends' additive distribution of NPs is homogeneous, and SrTiO<sub>3</sub>/CoO NPs form a continuous network inside the PEO/PVA blend at a concentration of 4 wt.%. The pressure-sensor application results with PEO/PVA/SrTiO<sub>3</sub>/CoO NCs show that the electrical capacitance ( $C_p$ ) increases with rise in applied pressure; this behaviour make it suitable for many electronic and electrical applications. In addition, the NCs with high linear attenuation coefficients have  $\gamma$ -ray source Cs-137. It is also used to protect against radiation. As the concentration of SrTiO<sub>3</sub>/CoO NPs increases, the transmissive radiation decreases and the attenuation coefficients increase. The results indicate that the PEO/PVA/SrTiO<sub>3</sub>/CoO NCs can be considered as excellent materials for pressure sensors and  $\gamma$ -ray shielding.

Наноккомпозити (НК) використовуються, як правило, для різних сфер промислового застосування, які вимагають мінімальних витрат і ваги. У цьому дослідженні наночастинки (НЧ) триоксиду Стронцію–Титану (SrTiO<sub>3</sub>)/оксиду Кобальту (CoO) поєднуються з сумішшю полімерів оксиду поліетилену (ПЕО)/полівінілового спирту (ПВС) для створення НК. Плівки виготовляються за допомогою процесу лиття, а в полімерну суміш додаються різні вагові відсотки SrTiO<sub>3</sub>/CoO НЧ (0, 1, 2, 3 і 4 мас.%). Сканівна електронна мікроскопія показує поверхні плівок ПЕО/ПВС/SrTiO<sub>3</sub>/CoO НК з декількома хаотично розподіленими агрегатами або фрагментами на

верхній поверхні послідовно та когерентно. Зображення оптичного мікроскопа демонструють, що адитивний розподіл НЧ у сумішах є однорідним, а  $\text{SrTiO}_3/\text{CoO}$  НЧ утворюють безперервну мережу всередині суміші ПЕО/ПВС за концентрації у 4 мас.%. Результати застосування датчика тиску з ПЕО/ПВС/ $\text{SrTiO}_3/\text{CoO}$  НК показують, що електрична ємність ( $C_p$ ) зростає зі збільшенням прикладеного тиску; така поведінка робить його придатним для багатьох електронних та електричних застосувань. Крім того, НК з високими коефіцієнтами лінійного згасання мають джерело  $\gamma$ -променювання Cs-137. Також його використовують для захисту від радіації. Зі збільшенням концентрації  $\text{SrTiO}_3/\text{CoO}$  НЧ пропускання випромінювання зменшується, а коефіцієнти послаблення збільшуються. Результати вказують на те, що ПЕО/ПВС/ $\text{SrTiO}_3/\text{CoO}$  НК можна розглядати як відмінні матеріали для давачів тиску й екранування  $\gamma$ -променів.

**Key words:** nanocomposites,  $\text{SrTiO}_3/\text{CoO}$  nanoparticles, pressure sensors,  $\gamma$ -ray shielding.

**Ключові слова:** нанокompозити, наночастинки  $\text{SrTiO}_3/\text{CoO}$ , датчики тиску, екранування  $\gamma$ -променів.

*(Received 31 March, 2023)*

## 1. INTRODUCTION

The production of novel polymers, mixes, composites, and sophisticated materials now necessitates altered mechanical, electric, optical, and thermal properties in order to match the required specifications [1, 2]. The development is taking place concurrently with a number of thorough researches designed to clarify the structure-property link of the modified materials. Prior to being manufactured, new polymeric films must be characterized optically, electrically, and thermally. The polarizers, absolute reflectors, optical filters, and narrow bandwidth filters are all examples of applications for transparent film. The usage of dielectric material films is successful in several optical equipment and materials [3, 4].

A new class of NCs' materials have been developed as a result of the interaction between macro- and nanocomposites for use in medical, biological, industrial, and defence applications. Since industrial, electronic, and communication technologies are now more often used for military and scientific purposes, electromagnetic interference (EMI) has emerged as the primary problem. The instruments' performance is compromised, and its lifespan is shortened by EMI from magnets. In order to prevent electromagnetic radiation from penetrating a shield, a material must either reflect or absorb the radiation. EMI shielding materials becoming lighter are needed to keep the pace of activity flowing. Although metals are frequently employed as electromagnetic protection materials, there are several drawbacks to metals, including

their high cost, heavy loading, poor adherence, propensity to corrode in severe conditions, and poor process ability [5, 6]. Even yet, due to concrete drawbacks, it is not always the best choice for  $\gamma$ -radiation safety. The alternate method of replacing it with material that has better mechanical strength, transfer, and no degradable qualities is to utilize material that has no visibility and has strong mechanical strength under adverse environmental circumstances [7, 8].

Additionally, adding metal to the polymer matrix enhances its mechanical, electrical, and thermal stability. Due to their unique physical, mechanical, and antibacterial characteristics, metal-polymer NCs, particularly, PVA NCs, are fascinating useful materials in many different sectors [9, 10]. The most intriguing foundation material is polyethylene oxide (PEO), which has a high level of chemical and thermal resilience. PEO is a semi crystalline polymer that, at ambient temperature, may exist in both amorphous and crystalline states. One of the most significant modern methods for creating novel polymeric materials is polymer mixing, which is also a practical method for creating materials with a wide range of characteristics [11, 12]. The indirect semiconductor material strontium titanate (SrTiO<sub>3</sub>) is regarded as one of the most significant photocatalysts because of its superior thermal and photo corrosion resistance capabilities. CoO is very helpful and stable in the industry, and when added to polymers, it develops optical and mechanical properties connected to its strong interfacial communication linking the organic and inorganic components [13, 14].

When radiation particles fall on matter, the energy of these particles is gradually transmitted to matter through collisions with atoms of matter until they stop. Because of these collisions, the atoms of the substance are ionized, *i.e.*, the electron is completely separated from its atom. The ways for  $\gamma$ -ray energy loss are varying in matter, photoelectric effect, pair production and the Compton effect. A  $\gamma$ -photon interacts with one of the electrons in the inner levels of the atom (with electrons in the last orbit of the atom). In this interaction, the beam is dispersed. When it is fallen one, its direction is changed, and its energy decreases [15, 16].  $\gamma$ -rays and x-rays have many applications in military, medical, health, scientific, and agricultural industries. Increasing the utilization of hazardous radiations, including  $\gamma$ -sources in hospitals and research centres for diagnostic and therapeutic applications, has provided a much more unsecured place for personnel. Therefore, there will be a need to design an appropriate shield [17, 18]. The purpose of this study is to create PEO/PVA/SrTiO<sub>3</sub>/CoO NCs for low-cost and lightweight pressure sensors and  $\gamma$ -ray shielding.

## 2. MATERIALS AND METHODS

By dissolving PEO/PVA in distilled water (40 ml) while employing a

magnetic stirrer for 40 minutes at temperature 70°C, the NCs were created. In concentrations of 0, 1, 2, 3, and 4 wt.%, the SrTiO<sub>3</sub>/CoO NPs were introduced to the polymer mix solution. In order to create the NCs' samples, casting method was used.

Using a scanning electron microscope, the surface morphology of PEO/PVA/SrTiO<sub>3</sub>/NiO NCs. Dual Bruker Flash EDS detectors and Bruker flash HD EBSD (Czech Tuscan Instrument Co.) are included in the Tuscan Mira3 SEM microscope for analytical research. The samples test in different concentrations by using an Olympus type Nikon-73346 optical microscope with a magnifying power of ×10 and equipped with a camera for microscopic photography.  $\gamma$ -ray shielding studies of PEO/PVA/SrTiO<sub>3</sub>/CoO NCs were carried out to examine the  $\gamma$ -ray attenuation characteristics for samples with various concentrations of SrTiO<sub>3</sub>/CoO NPs. The film of PEO/PVA/SrTiO<sub>3</sub>/CoO NCs is positioned at a distance of 1 cm from the  $\gamma$ -ray source (Cs-137-5mci), which is located at a distance of 2 cm from the detector. The Geiger counter is used to detect the transmitted  $\gamma$ -ray fluxes through the samples and determine the linear attenuation coefficients. Using a locally produced LCR meter of the HIOKI 3532-50 LCR HI TESTER type, the capacitance for various applied loads in the range of 80–160 bars is measured at 100 Hz.

The following equation may be used to get the linear attenuation coefficients ( $\mu$ ) from the material thicknesses [19]:  $N = N_0 e^{-\mu x}$ , where  $N_0$

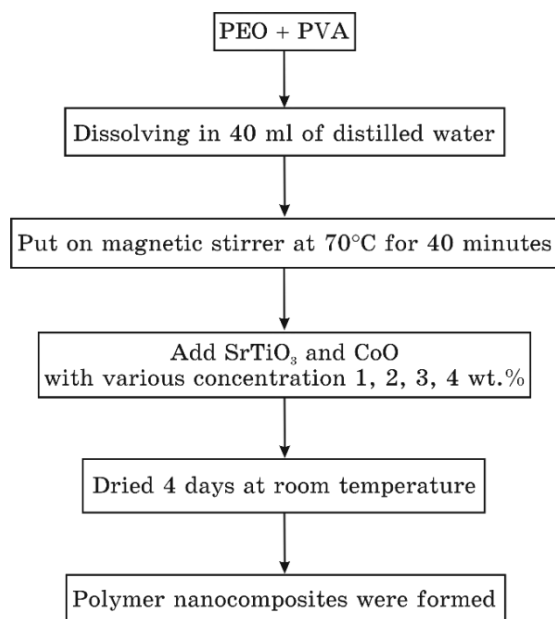


Fig. 1. Scheme of the PEO/PVA/SrTiO<sub>3</sub>/NiO NCs' synthesizing process.

is an incident  $\gamma$ -ray number;  $N$  is the attenuation of the  $\gamma$ -rays, and  $x$  is the thickness.

### 3. RESULTS AND DISCUSSION

#### 3.1. Scanning Electron Microscopy (SEM) Measurements of PEO/PVA/SrTiO<sub>3</sub>/CoO NCs

The impacts of SrTiO<sub>3</sub>/CoO NPs' concentration and the dispersion of NCs' particles in the polymer matrix are examined using SEM. Figure 2 displays typical SEM images of the PEO/PVA blend with and without various SrTiO<sub>3</sub>/CoO NPs' concentrations. It is discovered that image *a* for an undoped polymer combination is softer, more homogenous, and more coherent. When SrTiO<sub>3</sub>/CoO NPs are introduced to the PEO/PVA blend, the SrTiO<sub>3</sub>/CoO surface changes, becoming rougher and containing some tiny aggregate particles (white spot) (see image *b*). This work showed the organic surface modification of the SrTiO<sub>3</sub>/CoO NPs as result of an adhesion between the surface of the SrTiO<sub>3</sub>/CoO NPs and the polymer matrix as the SrTiO<sub>3</sub>/CoO level climbs to 1 wt.% [20, 21]. As the concentration of SrTiO<sub>3</sub>/CoO rises, white patches on the backscattered images seem to indicate clusters of SrTiO<sub>3</sub>/CoO NPs. The coarse spherulite structure in the image is caused by SrTiO<sub>3</sub>/CoO segregating into the blend's areas (image *c*). The hills that resemble ganglia in image *d*, also known as the longitudinal form image, are smooth with few creases (image *e*) [22–25]. Figure 3 shows particles' size for PEO/PVA/SrTiO<sub>3</sub>/CoO NCs calculated from SEM analysis.

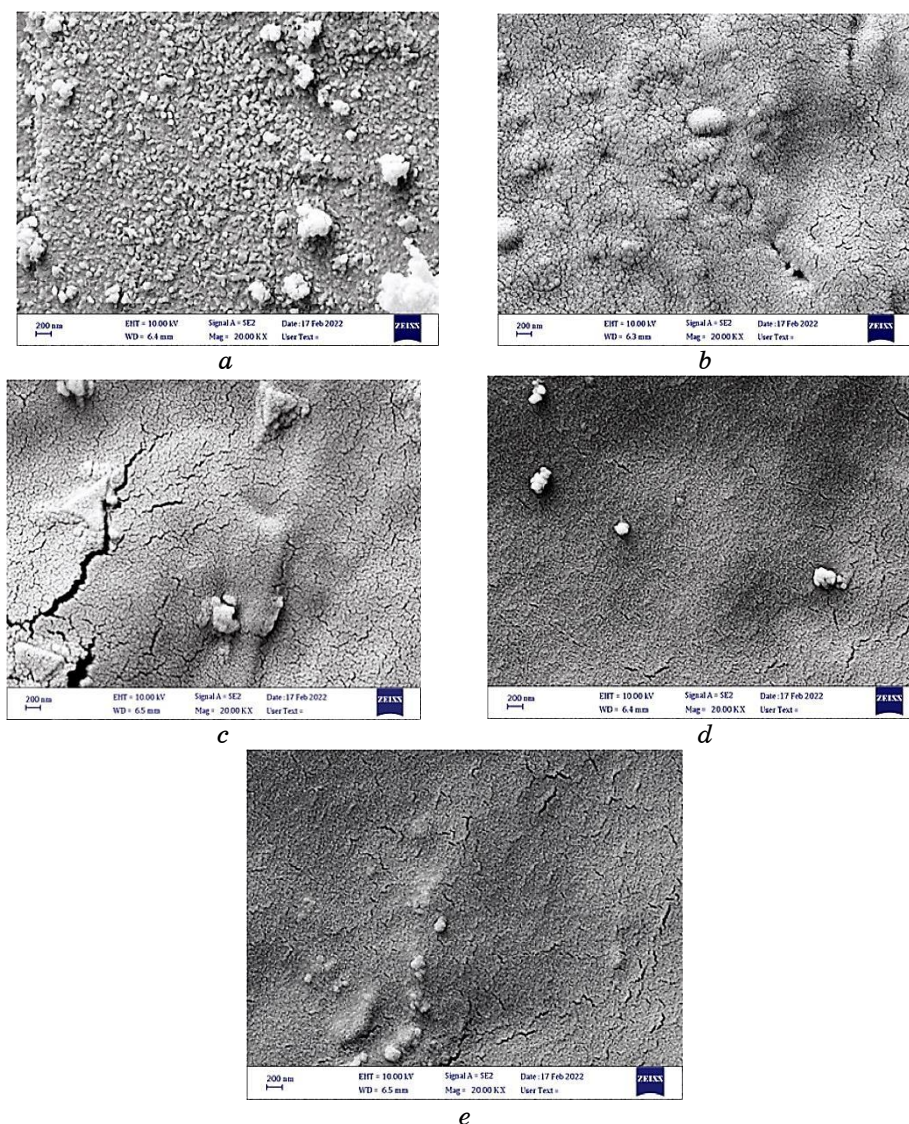
#### 3.2. Optical Microscopy for PEO/PVA/SrTiO<sub>3</sub>/CoO Nanocomposites

Figure 4 shows the photomicrographs of the NCs made of PEO/PVA/SrTiO<sub>3</sub>/CoO. At lower concentrations, the SrTiO<sub>3</sub>/CoO NPs are clustered together as seen in the images (*a*, *b*, *c*, *d* and *e*). SrTiO<sub>3</sub>/CoO NPs create a continuous network inside the PEO/PVA mixture at a concentration of 4 wt.% for NCs as the concentration of NPs increases [26–29].

#### 3.3. Application of PEO/PVA/SrTiO<sub>3</sub>/CoO NCs for Pressure Sensors

Figure 5 depicts how pressure affects the electrical capacitance of PEO/PVA/SrTiO<sub>3</sub>/CoO NCs. This figure shows that as the pressure is increased, the electrical capacitance of NCs rises.

A crystalline area with an internal dipole moment is assigned to the NCs' samples in the explanation of the electrical capacitance behaviour for NCs under pressure. In the absence of any mechanical or electrical



**Fig. 2.** SEM images (200 μm) for PEO/PVA/SrTiO<sub>3</sub>/CoO NCs: (a) for PEO/PVA; (b) for 1 wt.% SrTiO<sub>3</sub>/CoO; (c) for 2 wt.% SrTiO<sub>3</sub>/CoO; (d) for 3 wt.% SrTiO<sub>3</sub>/CoO; (e) for 4 wt.% SrTiO<sub>3</sub>/CoO.

activities, these dipole moments are orientated randomly, and the net dipole moment is zero.

An electric field is created as soon as pressure is applied because the local dipole distributions are altered. The charges at the top and bottom of the samples are gathered by generating an electric field [30–34].

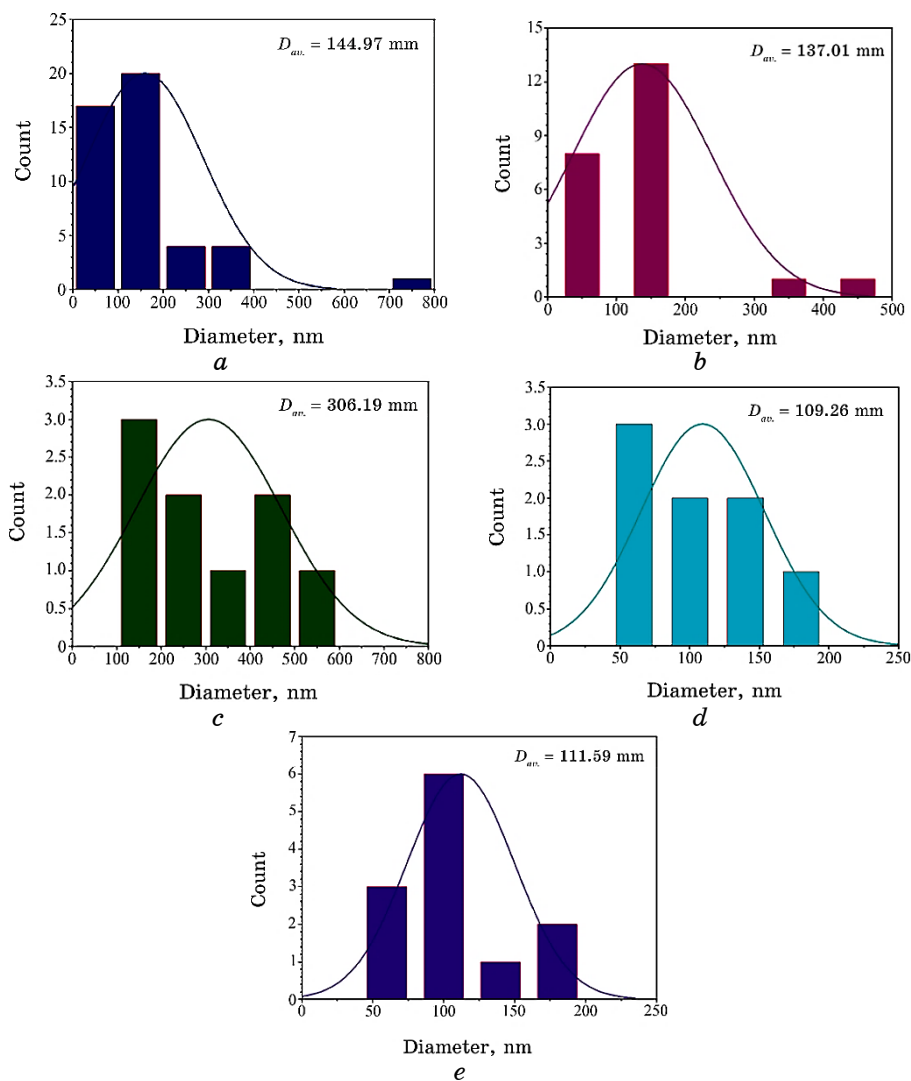


**Fig. 3.** Particles' size for PEO/PVA/SrTiO<sub>3</sub>/CoO NCs: (a) for PEO/PVA; (b) for 1 wt.% SrTiO<sub>3</sub>/CoO; (c) for 2 wt.% SrTiO<sub>3</sub>/CoO; (d) for 3 wt.% SrTiO<sub>3</sub>/CoO; (e) for 4 wt.% SrTiO<sub>3</sub>/CoO.

Figure 6 shows the electrical capacitance of PEO/PVA/SrTiO<sub>3</sub>/CoO NCs influenced by the concentration of SrTiO<sub>3</sub>/CoO NPs. When the concentration of SrTiO<sub>3</sub>/CoO NPs increases, the electrical capacitance of NCs increases. Higher concentrations of SrTiO<sub>3</sub>/CoO NPs are connected with an increase in electrical capacitance, which is due to an increase in charge carriers [35–37].

Figure 7 illustrates how SrTiO<sub>3</sub>/CoO NPs affect the sensitivity for

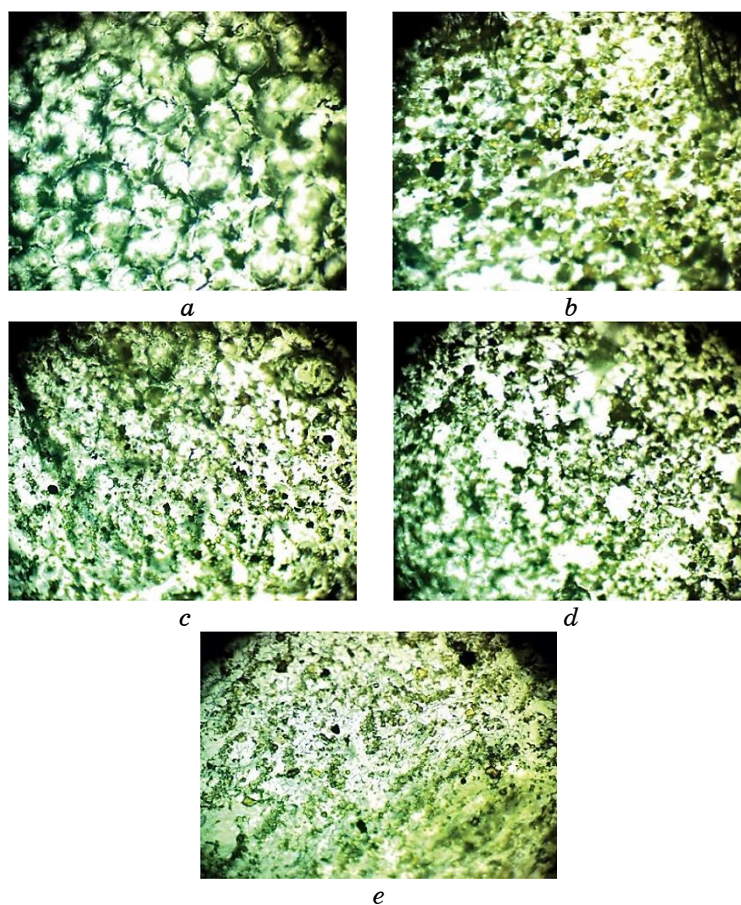


**Fig. 4.** Photomicrographs ( $\times 10$ ) for PEO/PVA/SrTiO<sub>3</sub>/CoO NCs: (a) for PEO/PVA; (b) for 1 wt.% SrTiO<sub>3</sub>/CoO; (c) for 2 wt.% SrTiO<sub>3</sub>/CoO; (d) for 3 wt.% SrTiO<sub>3</sub>/CoO; (e) for 4 wt.% SrTiO<sub>3</sub>/CoO.

PEO/PVA/SrTiO<sub>3</sub>/CoO NCs. This graph shows that, due to the internal dipole moment, the sensitivity of NCs rises as the concentration of SrTiO<sub>3</sub>/CoO NPs increases [38–40].

### 3.4. Application of PEO/PVA/SrTiO<sub>3</sub>/CoO NCs for $\gamma$ -Ray Shielding

The change of  $N/N_0$  in the PEO/PVA mixture with various SrTiO<sub>3</sub>/CoO NPs' concentrations is shown in Fig. 8. As SrTiO<sub>3</sub>/CoO NPs' concentrations rise,  $N/N_0$  decreases. This is due to an increase in attenuation radiation, which causes the transmission radiation to fall [41–44]. Figure 9 shows increasing  $\ln(N/N_0)$  for PEO/PVA mixture with increasing SrTiO<sub>3</sub>/CoO NPs' concentration.

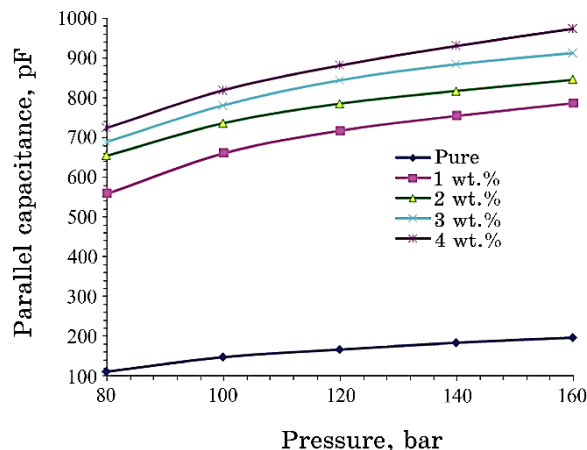


Fig. 5. Dependence of parallel capacitance of PEO/PVA/SrTiO<sub>3</sub>/CoO NCs on pressure.

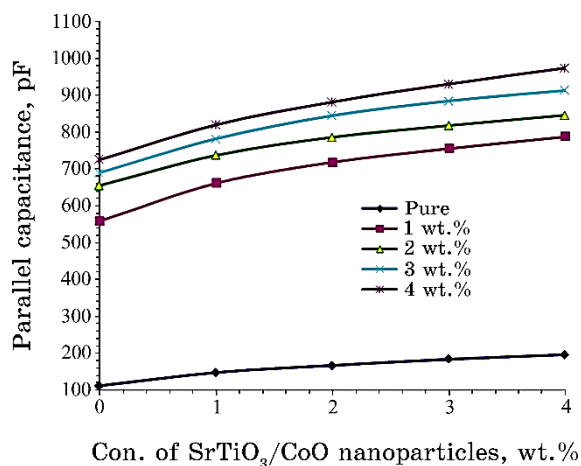
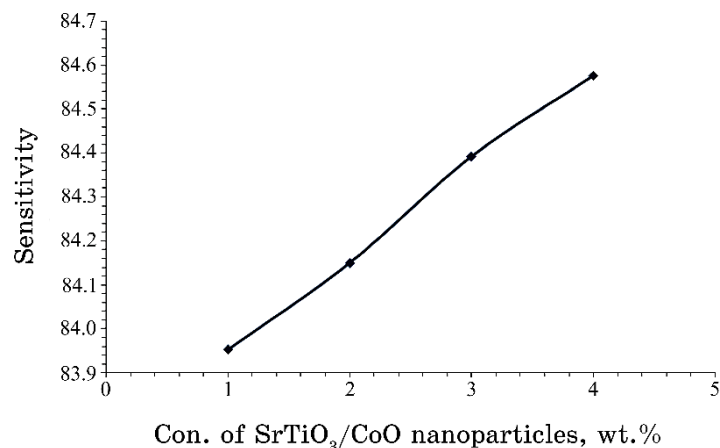


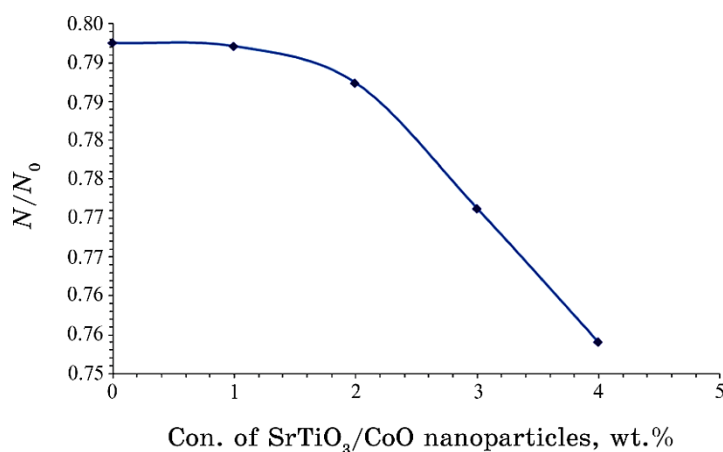
Fig. 6. Effect of SrTiO<sub>3</sub>/CoO NPs' concentrations on parallel capacitance for PEO/PVA/SrTiO<sub>3</sub>/CoO NCs at 80 bars.

Figure 10 demonstrates the relationship between the concentrations of SrTiO<sub>3</sub>/CoO NPs and  $\gamma$ -radiation attenuation coefficients. Due to the shielding materials in NCs either absorbing or reflecting  $\gamma$ -radiation, the coefficient of attenuation increases as the concentration of NPs does. The findings obtained by concrete and polymer NCs were generally comparable; however, the latter has an advantage over the former due to its mobility, lack of electrical characteristics, and capacity to inhibit neutron emission [45–47].

Figure 11 demonstrates the mass attenuation coefficient of  $\gamma$ -



**Fig. 7.** The influence of SrTiO<sub>3</sub>/CoO NPs' concentration on sensitivity for PEO/PVA/SrTiO<sub>3</sub>/CoO NCs.



**Fig. 8.** Dependence of  $N/N_0$  for PEO/PVA mixture on SrTiO<sub>3</sub>/CoO NPs' concentration.

radiation as a function of concentration of SrTiO<sub>3</sub>/CoO NPs. Due to the fact that shielding materials built of NCs either absorb or reflect  $\gamma$ -rays [48, 49], it can be seen from this figure that the mass attenuation coefficient increases as NPs' concentration increases.

#### 4. CONCLUSIONS

This work aims to prepare of polyethylene oxide (PEO)/polyvinyl alcohol (PVA) polymer blend doped with strontium–titanium trioxide

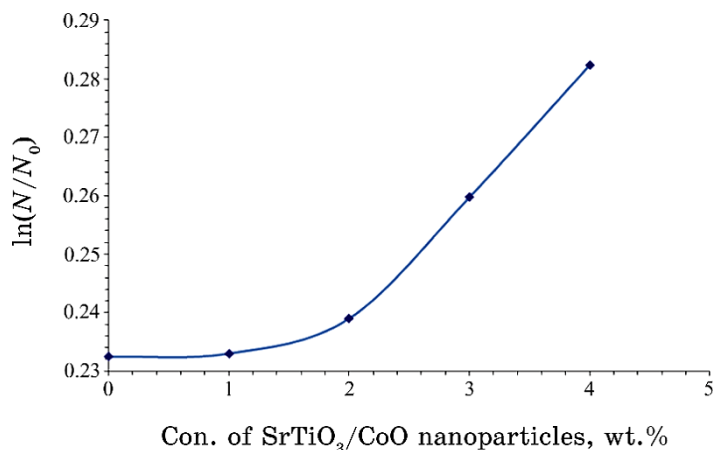


**Fig. 9.** Variance of  $\ln(N/N_0)$  for PEO/PVA mixture with different concentrations of SrTiO<sub>3</sub>/CoO NPs.

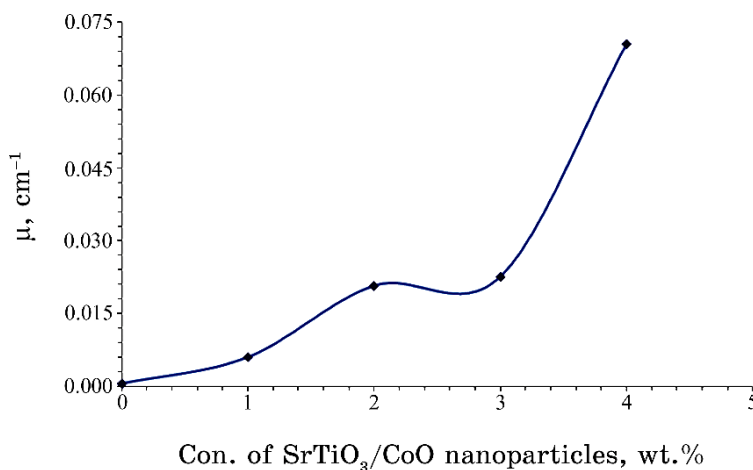


**Fig. 10.** Difference of attenuation coefficients of  $\gamma$ -radiation for PEO/PVA mixture with different concentrations of SrTiO<sub>3</sub>/CoO NPs.

(SrTiO<sub>3</sub>) and cobalt oxide (CoO) as new NCs, which can be utilized in different nanodevices with few cost, lightweight, excellent properties, good mechanical and chemical characteristics.

The surfaces of the PEO/PVA/SrTiO<sub>3</sub>/CoO NCs' films are shown by scanning electron microscopy to have many randomly dispersed aggregation or pieces on the top surface, which are consistent and coherent. The optical microscope photos demonstrate that a continuous network of SrTiO<sub>3</sub>/CoO NPs forms inside the polymers, when the proportion is of 4 wt.%. The PEO/PVA/SrTiO<sub>3</sub>/CoO NCs pressure-sensor applica-

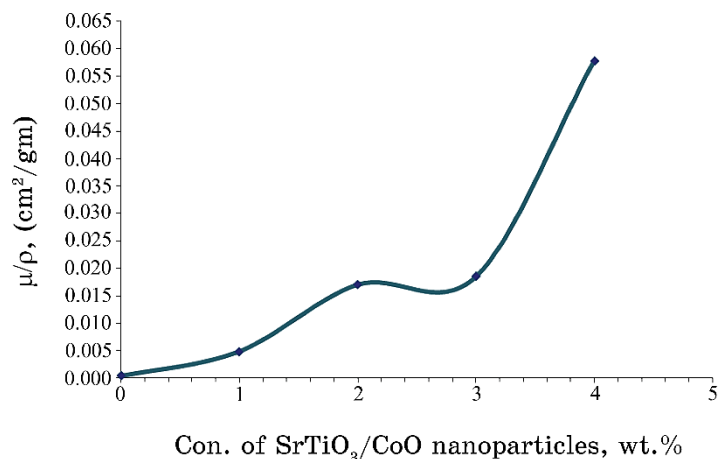


**Fig. 11.** Variation of mass attenuation coefficient of PEO/PVA mixture with different concentrations of SrTiO<sub>3</sub>/NiO NPs.

tion findings show that the electrical capacitance ( $C_p$ ) rises with the rise in applied pressure. The results of application for  $\gamma$ -ray shielding in NCs demonstrated that the transmission radiation reduces as the concentration of SrTiO<sub>3</sub>/CoO NPs rises; on the other hand, the attenuation coefficients rise as the concentration of SrTiO<sub>3</sub>/CoO NPs rises. The results of PEO/PVA/SrTiO<sub>3</sub>/CoO nanostructures' applications indicated that the nanostructures' films are highly sensitive for pressure and excellent for  $\gamma$ -ray shielding.

## REFERENCES

1. Morget Martin, Neena Prasad, Muthu Mariappan Sivalingam, D. Sastikumar, and Balasubramanian Karthikeyan, *J. Mater. Sci.: Mater. Electron.*, **29**: 365 (2018); doi:10.1007/s10854-017-7925-z
2. P. Vasudevan, S. Thomas, K. Arunkumar, S. Karthika, and N. Unnikrishnan, *Journal of Materials, Science and Engineering*, **73**: 1 (2015); doi:10.1088/1757-899X/73/1/012015
3. A. A. Mohammed and M. A. Habeeb, *Silicon*, **15**: 5163 (2023); <https://doi.org/10.1007/s12633-023-02426-2>
4. G. Aras, E. L. Orhan, I. F. Selçuk, S. B. Ocak, and M. Ertuğrul, *Procedia-Social and Behavioral Sciences*, **95**: 1740 (2015); <https://doi.org/10.1016/j.sbspro.2015.06.295>
5. M. A. Habeeb, *European Journal of Scientific Research*, **57**, No. 3: 478 (2011).
6. M. S. Aziz and H. M. El-Mallah, *International Journal of Polymeric Materials*, **54**, No. 12: 1157 (2005); <https://doi.org/10.1080/009140390901680>
7. M. A. Habeeb and Z. S. Jaber, *East European Journal of Physics*, **4**: 176 (2022); doi:10.26565/2312-4334-2022-4-18
8. K. Sardar, R. Bounds, M. Carravetta, G. Cutts, J. S. Hargreaves, A. L. Hector,

- and F. Wilson, *Dalton Transactions*, **45**, No. 13: 5765 (2016); <https://doi.org/10.1039/C5DT04961J>
9. A. H. Hadi and Majeed Ali Habeeb, *Journal of Mechanical Engineering Research and Developments*, **44**, No. 3: 265 (2021); <https://jmerd.net/03-2021-265-274>
  10. N. Manavizadeh, A. Khodayari, and E. Asl-Soleimani, *Proceedings of ISES World Congress (2008)*, vol. **1**, p. 1120; [https://doi.org/10.1007/978-3-540-75997-3\\_220](https://doi.org/10.1007/978-3-540-75997-3_220)
  11. Q. M. Jebur, A. Hashim, and M. A. Habeeb, *Egyptian Journal of Chemistry*, **63**: 719 (2020); <https://dx.doi.org/10.21608/ejchem.2019.14847.1900>
  12. A. R. Farhadizadeh and H. Ghomi, *Materials Research Express*, **7**, No. 3: 36502 (2020); <https://doi.org/10.1088/2053-1591/ab79d2>
  13. S. M. Mahdi and M. A. Habeeb, *Optical and Quantum Electronics*, **54**, Iss. 12: 854 (2022); <https://doi.org/10.1007/s11082-022-04267-6>
  14. F. A. Modine, R. W. Major, T. W. Haywood, G. R. Gruzalski, and D. Y. Smith, *Physical Review B*, **29**, No. 2: 836 (1984); <https://doi.org/10.1103/PhysRevB.29.836>
  15. N. Hayder, M. A. Habeeb, and A. Hashim, *Egyptian Journal of Chemistry*, **63**: 577 (2020); [doi:10.21608/ejchem.2019.14646.1887](https://doi.org/10.21608/ejchem.2019.14646.1887)
  16. O. E. Gouda, S. F. Mahmoud, A. A. El-Gendy, and A. S. Haiba, *Indonesian Journal of Electrical Engineering*, **12**, No. 12: 7987 (2014); <https://doi.org/10.11591/telkomnika.v12i12.6675>
  17. M. A. Habeeb, A. Hashim, and N. Hayder, *Egyptian Journal of Chemistry*, **63**: 709 (2020); <https://dx.doi.org/10.21608/ejchem.2019.13333.1832>
  18. H. Shivashankar, A. M. Kevin, Pavankumar R. Sondar, M. H. Shrishail, and S. M. Kulkarni, *J. Mater. Sci.: Mater. Electron.*, **32**: 28674 (2021); <https://doi.org/10.1007/s10854-021-07242-1>
  19. A. Hashim, M. A. Habeeb, and Q. M. Jebur, *Egyptian Journal of Chemistry*, **63**: 735 (2020); <https://dx.doi.org/10.21608/ejchem.2019.14849.1901>
  20. T. S. Praveenkumar, J. S. Ashwajeet, and R. Ramanna, *Journal of Polymers*, **2015**: Article ID 893148 (2015); <https://doi.org/10.1155/2015/893148>
  21. M. A. Habeeb and W. H. Rahdi, *Optical and Quantum Electronics*, **55**, Iss. 4: 334 (2023); <https://doi.org/10.1007/s11082-023-04639-6>
  22. M. Rezvanpour, M. Hasanzadeh, D. Azizi, A. Rezvanpour, and M. Alizadeh, *Mater. Chem. Phys.*, **215**: 299 (2018); <https://doi.org/10.1016/j.matchemphys.2018.05.044>
  23. S. M. Mahdi and M. A. Habeeb, *Physics and Chemistry of Solid State*, **23**, No. 4: 785 (2022); [doi:10.15330/pcss.23.4.785-792](https://doi.org/10.15330/pcss.23.4.785-792)
  24. J. B. Ramesh and K. K. Vijaya, *Chemtech*, **7**: 171 (2014); [https://sphinx.sai.com/2015/ch\\_vol7\\_no1/2/\(171-180\)%20014.pdf](https://sphinx.sai.com/2015/ch_vol7_no1/2/(171-180)%20014.pdf)
  25. M. A. Habeeb, W. S. Mahdi, *International Journal of Emerging Trends in Engineering Research*, **7**, No. 9: 247 (2019); [doi:10.30534/ijeter/2019/06792019](https://doi.org/10.30534/ijeter/2019/06792019)
  26. T. S. Soliman and S. A. Vshivkov, *J. Non-Cryst. Solids*, **519**: 119452 (2019); <https://doi.org/10.1016/j.jnoncrysol.2019.05.028>
  27. S. M. Mahdi and M. A. Habeeb, *AIMS Materials Science*, **10**, No. 2: 288 (2023); [doi:10.3934/mat.2023015](https://doi.org/10.3934/mat.2023015)
  28. S. Ahmad and S. A. Agnihotry, *Bull. Mater. Sci.*, **30**, No. 1: 31 (2007); <https://doi.org/10.1007/s12034-007-0006-9>
  29. M. A. Habeeb and R. S. Abdul Hamza, *Journal of Bionanoscience*, **12**, No. 3:

- 328 (2018); <https://doi.org/10.1166/jbns.2018.1535>
30. S. Ramesh and Liew Chiam Wen, *Ionics (Kiel)*, **16**, No. 3: 255 (2010); <https://doi.org/10.1007/s11581-009-0388-3>
31. M. A. Habeeb, A. Hashim, and N. Hayder, *Egyptian Journal of Chemistry*, **63**: 697 (2020); <https://dx.doi.org/10.21608/ejchem.2019.12439.1774>
32. Mojtaba Haghighi-Yazdi and Pearl Lee-Sullivan, *Journal of Applied Polymer Science*, **132**, Iss. 3: 41316 (2015); <https://doi.org/10.1002/app.41316>
33. N. K. Al-Sharifi and M. A. Habeeb, *Silicon*, **15**: 4979 (2023); <https://doi.org/10.1007/s12633-023-02418-2>
34. A. Goswami, A. K. Bajpai, and B. K. Sinha, *Polym. Bull.*, **75**, No. 2: 781 (2018); <https://doi.org/10.1007/s00289-017-2067-2>
35. M. A. Habeeb and W. K. Kadhim, *Journal of Engineering and Applied Sciences*, **9**, No. 4: 109 (2014); [doi:10.36478/jeasci.2014.109.113](https://doi.org/10.36478/jeasci.2014.109.113)
36. K. Rajesh, Vincent Crasta, N. B. Rithin Kumar, Gananatha Shetty, and P. D. Rekha, *Journal of Polymer Research*, **26**, No. 4: 99 (2019); <https://doi.org/10.1007/s10965-019-1762-0>
37. M. A. Habeeb, *Journal of Engineering and Applied Sciences*, **9**, No.4: 102 (2014); [doi:10.36478/jeasci.2014.102.108](https://doi.org/10.36478/jeasci.2014.102.108)
38. Goutam Chakraborty, Kajal Gupta, Dipak Rana, and Ajit Kumar Meikap, *Adv. Nat. Sci.: Nanosci. Nanotechnol.*, **4**, No. 2: 025005 (2013); <https://doi.org/10.1088/2043-6262/4/2/025005>
39. A. H. Hadi and M. A. Habeeb, *Journal of Physics: Conference Series*, **1973**, No. 1: 012063 (2021); [doi:10.1088/1742-6596/1973/1/012063](https://doi.org/10.1088/1742-6596/1973/1/012063)
40. S. Ju, M. Chen, H. Zhang, and Z. Zhang, *Journal of Express Polymer Letters*, **8**, No. 9: 682 (2014); <https://doi.org/10.3144/expresspolymlett.2014.71>
41. S. M. Mahdi and M. A. Habeeb, *Digest Journal of Nanomaterials and Biostructures*, **17**, No. 3: 941 (2022); <https://doi.org/10.15251/DJNB.2022.173.941>
42. O. Abdullah, G. M. Jamal, D. A. Tahir, and S. R. Saeed, *International Journal of Applied Physics and Mathematics*, **1**, No. 2: 101 (2011); <https://doi.org/10.7763/IJAPM.2011.V1.20>
43. Q. M. Jebur, A. Hashim, and M. A. Habeeb, *Egyptian Journal of Chemistry*, **63**, No. 2: 611 (2020); <https://dx.doi.org/10.21608/ejchem.2019.10197.1669>
44. Roshani N. Bhagat and Vijaya S. Sangawar, *Int. J. Sci. Res. (IJSR)*, **6**, Iss. 11: 361 (2017); <https://www.ijrsr.net/getabstract.php?paperid=ART20177794>
45. M. A. Habeeb and R. S. A. Hamza, *Indonesian Journal of Electrical Engineering and Informatics*, **6**, No. 4: 428 (2018); [doi:10.11591/ijeel.v6i1.511](https://doi.org/10.11591/ijeel.v6i1.511)
46. M. H. Dwech, M. A. Habeeb, and A. H. Mohammed, *Ukr. J. Phys.*, **67**, No. 10: 757 (2022); <https://doi.org/10.15407/ujpe67.10.757>
47. R. Dalven and R. Gill, *J. Appl. Phys.*, **38**, No. 2: 753 (1967); [doi:10.1063/1.1709406](https://doi.org/10.1063/1.1709406)
48. S. M. Mahdi and M. A. Habeeb, *Polymer Bulletin*, **80**: 12741 (2023); <https://doi.org/10.1007/s00289-023-04676-x>
49. C. C. Okpala, *Int. J. Eng. Res. Dev.*, **8**, No. 11: 17 (2013).